Sensors and Materials, Vol. 19, No. 7 (2007) 435–444
MYU Tokyo

S & M 0694

Optical Characteristics of an N-Well/Gate-Tied PMOSFET-type Photodetector with Built-in Transfer Gate for CMOS Image Sensor

Sang-Ho Seo, Kyoung-Do Kim, Min-Woong Seo, Jae-Sung Kong, Jang-Kyoo Shin* and Pyung Choi

Department of Electronics, Kyungpook National University,
1370 Sankyuk-dong, Buk-ku, Daegu, 702-701, Korea

(Received July 4, 2007; accepted September 27, 2007)

Key words: photodetector, PMOSFET, built-in transfer gate, CMOS image sensor

In this study, a new n-well/gate-tied p-channel metal-oxide-semiconductor field-effect transistor (PMOSFET)-type photodetector with a built-in transfer gate has been designed and fabricated using 0.35 μm standard complementary metal oxide semiconductor (CMOS) technology. This photodetector is composed of a floating gate that is tied to an n-well and a built-in transfer gate. The built-in transfer gate controls the photocurrent flow by controlling the barrier for holes in the proposed photodetector. The designed and fabricated photodetector exhibits I_{DS}-V_{DS} characteristics that are similar to those of a general MOSFET when the incident light power, instead of the gate voltage, is varied. The area of the proposed photodetector is 3.8 × 5.7 μm and the responsivity is greater than 2.5 × 10^2 A/W, at a wavelength of 633 nm.

1. Introduction

The photodetector is a very important device that can be used as an image sensor in charge-coupled devices (CCDs) and CMOS image sensors (CISs).(1,2) Photodetectors, which are widely used as an image sensor in CISs, include charge modulation devices (CMDs), pinned photodiodes, hole accumulation diodes (HADs), avalanche photodiodes, metal-semiconductor-metal photodetectors (MSM-PDs) and silicon-on-insulator (SOI) photodetectors.(1–9) These devices, however, have many advantages and disadvantages. Regarding CISs, photodetectors are fabricated by standard CMOS technology. If the structure of the photodetector is not compatible with the standard CMOS technology, the photodetector cannot be fabricated with the driving circuit on the same chip.

*Corresponding author: e-mail: jkshin@ee.knu.ac.kr

In addition, the issue of CIS technology affects the dynamic range and photosensitivity of the photodetector. Since the application area of the CIS is very broad, a wide dynamic range and a high level of photosensitivity are essential in order to obtain high image quality. The p-n junction photodiode that is used in commercial CIS products has a good dynamic range but low photosensitivity. On the other hand, the high-gain photodetector has a high level of photosensitivity but a narrow dynamic range. In conventional technology, the use of a high-gain photodetector and an additional transfer MOSFET is necessary to control photosensitivity levels. The integration density of the CIS, however, is low because of the use of the additional transfer MOSFET.[1,2]

In this paper, an n-well/gate-tied PMOSFET-type photodetector with a built-in transfer gate that has a high and variable photosensitivity without the additional transfer MOSFET has been proposed. This photodetector was designed and fabricated using 2-poly 4-metal 0.35 μm standard CMOS technology and its optical responses were measured.

2. N-well/Gate-Tied PMOSFET-Type Photodetector with a Built-in Transfer Gate and Its Characteristics

Figure 1 shows a cross-sectional view of the conventional PMOSFET-type photodetector.[9] The structure is similar to that of the floating-gate/body-tied PMOSFET photodetector. The operational principle of this photodetector is as follows:[9] a built-in field, induced by the n^+-polysilicon gate and the n-well, separates the photogenerated electron-hole pairs (EHPs). The holes drift toward the channel and are swept into the drain. The electrons, on the other hand, effectively accumulate in the body because of the barrier, which has a higher potential than that of the holes. These accumulated electrons reduce the potential barrier of holes that flow from the source to the drain and

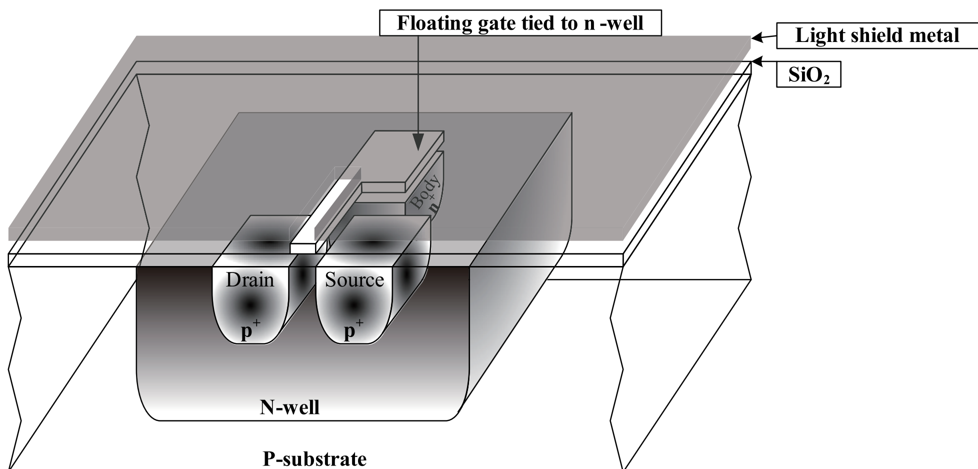

Fig. 1. Cross-sectional view of the conventional PMOSFET-type photodetector.

are fed back to the gate through the gate/body connection, acting as a negative gate voltage. Thus, the photocurrent is highly amplified.

If this photodetector is used in the 3-transistor (3-Tr.) active pixel sensor (APS), a noise reduction circuit, for example, a correlated double sampling (CDS) circuit, is not easily implementable without a frame memory. On the other hand, if this photodetector is used in the 4-transistor (4-Tr.) APS, a larger pixel size than that of the 3-Tr. APS is required because of the transfer MOSFET.

Figure 2 shows a cross-sectional view of the proposed photodetector. The structure is similar to that of the conventional PMOSFET-type photodetector, but the proposed photodetector has another gate that can control the generated photocurrent. Figure 3 shows the energy band diagram of the proposed photodetector. The operation principle of the proposed photodetector is similar to that of the conventional PMOSFET-type photodetector. If the bias of the built-in transfer gate is positive (Fig. 3(a)), the energy level is lower under the transfer gate. On the other hand, if the bias of the built-in transfer gate is negative (Fig. 3(b)), the energy level is higher under the built-in transfer gate. This means that the built-in transfer gate controls the photocurrent flow by controlling the barrier for the holes, depending on the applied bias. Moreover, if the proposed photodetector is used in the 3-Tr. APS, the structure of the pixel using the proposed photodetector is basically that in the 3-Tr. APS, but its function is the same as that in the 4-Tr. APS, because the built-in transfer gate of the proposed photodetector has the same function as that in the transfer MOSFET of the 4-Tr. APS. Therefore, the pixel using the proposed photodetector has merits such as a smaller area and less interference from the MOSFETs compared with that in the conventional 4-Tr. APS. A noise reduction circuit such as the CDS circuit can also be easily implemented without a frame memory. Figure 4 shows the schematic symbol and the layout of the proposed photodetector. The area of the proposed photodetector is 3.8 × 5.7 µm.

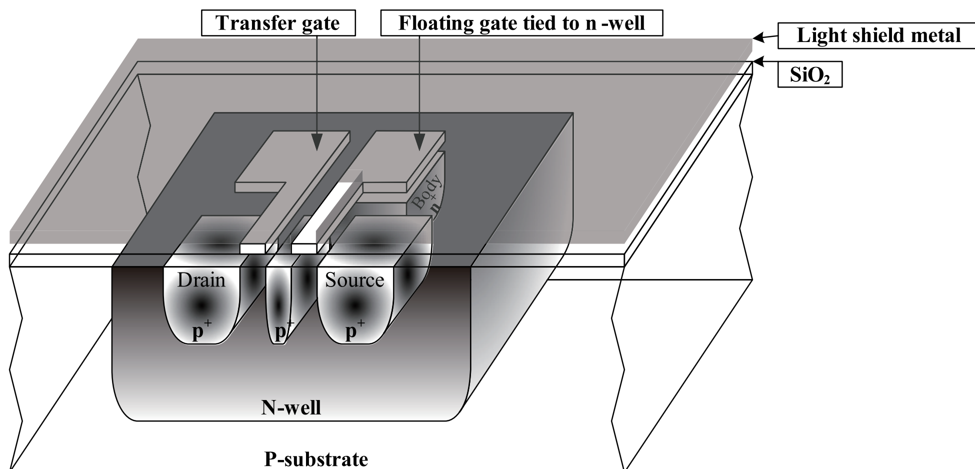

Fig. 2. Cross-sectional view of the proposed photodetector.

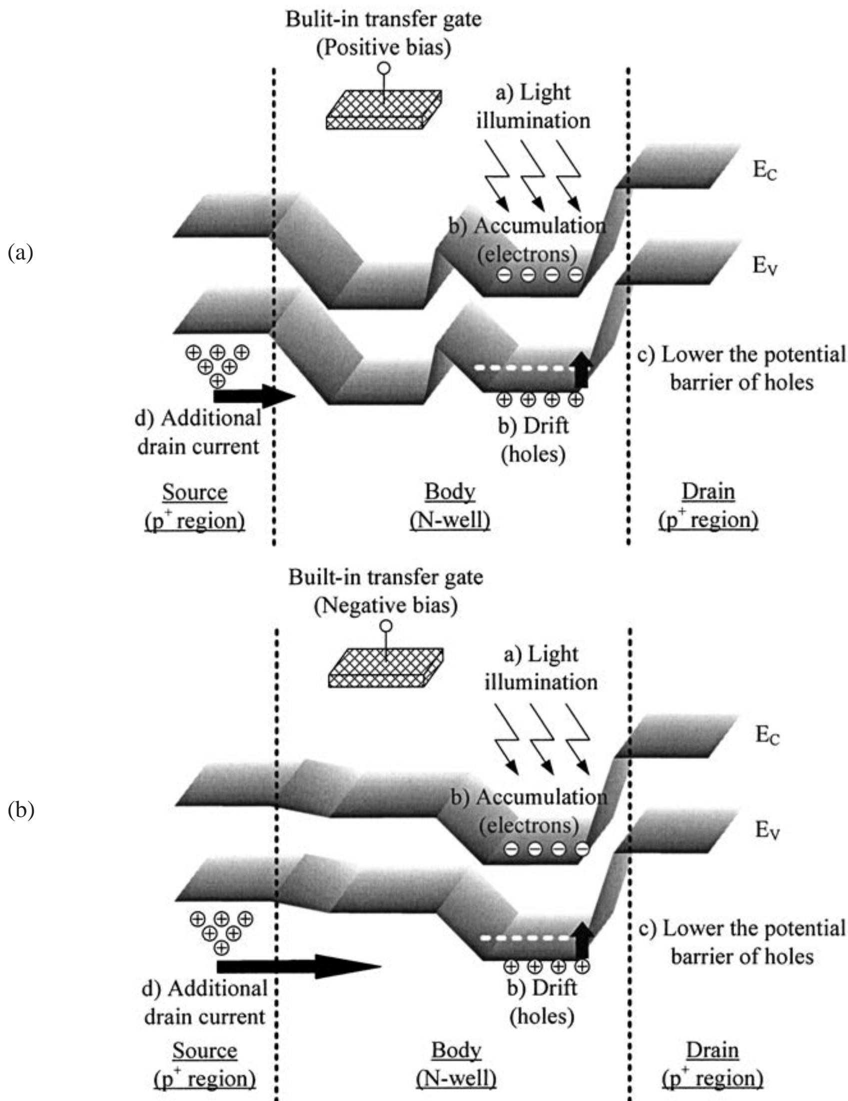

Fig. 3. Energy band diagram of the proposed photodetector: (a) bias of the built-in transfer gate is positive and (b) bias of the built-in transfer gate is negative.

3. Results and Discussion

To optimize the operating voltage of the built-in transfer gate in the proposed photodetector, we measured the variation of the drain current (I_{DS}) with the drain voltage (V_{DS}) as a function of the built-in transfer gate (V_{TG}) bias level. Figure 5 shows

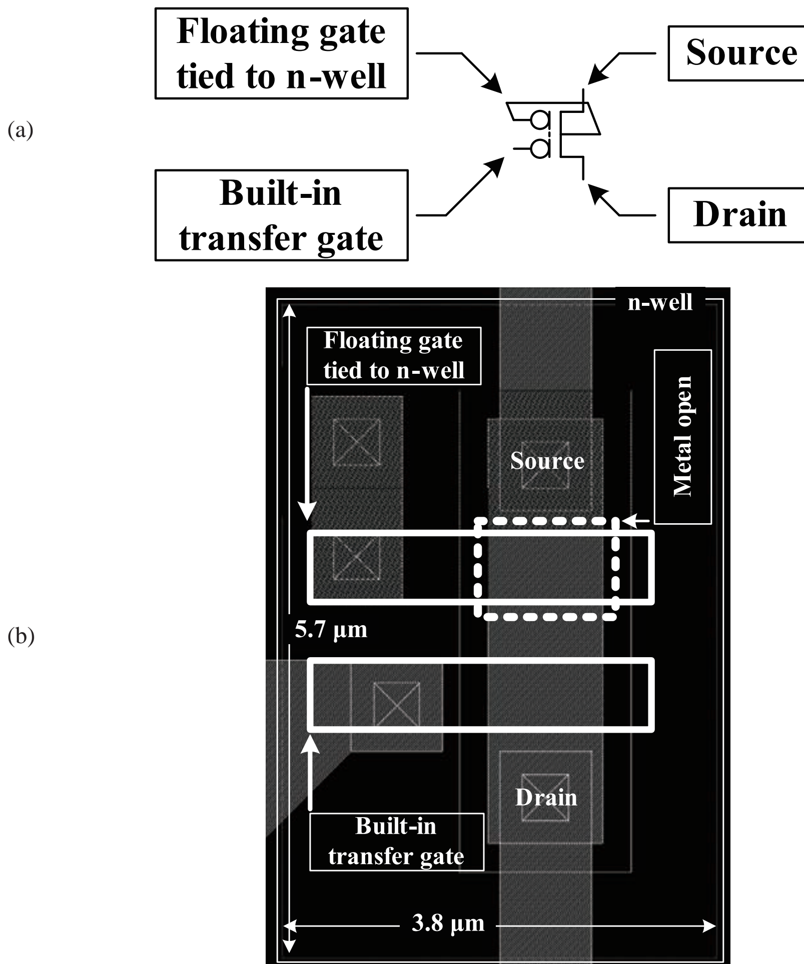

Fig. 4. Proposed photodetector: (a) schematic symbol and (b) layout.

the measurement results. The light source used in the experiment was a He-Ne laser (wavelength = 633 nm). The proposed photodetector, fabricated by a 0.35 µm standard CMOS process, is operated using a 3.3 V power supply (V_{DD}). Therefore, the bias voltage of the built-in transfer gate varied between 0 V (GND) and 3.3 V (V_{DD}). From this figure, we can confirm that for an optimized positive bias voltage of the built-in transfer gate, the minimum photocurrent is 3.3 V (V_{DD}), while for an optimized negative bias voltage of the built-in transfer gate, the maximum photocurrent is 0 V (GND). Also, we can confirm that this result agrees with the operational principle of the built-in transfer gate, as mentioned in the previous section.

Figure 6 shows the variation of the drain current (I_{DS}) with the drain voltage (V_{DS}) as a function of the incident-light power. The light source is the same as that in the

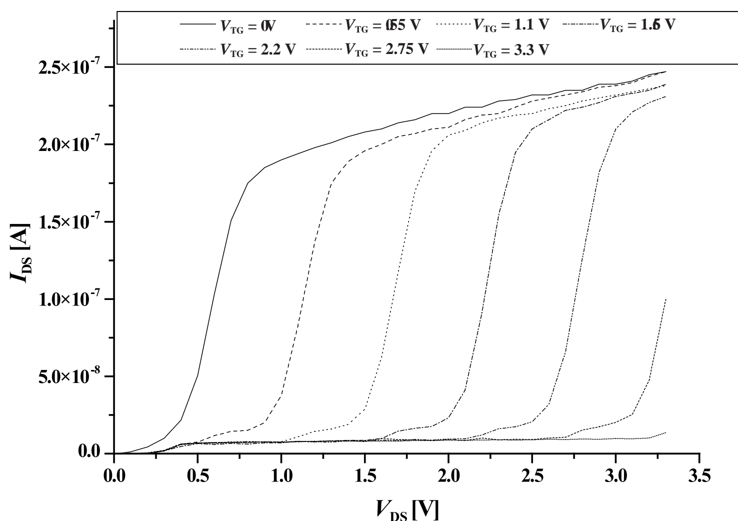

Fig. 5. Variation of the drain current (I_{DS}) with the drain voltage (V_{DS}) as a function of the built-in transfer gate (V_{TG}) bias level.

previous experiment. Between the floating gate and the built-in transfer gate, a p^+ diffusion region exists. It is possible to interrupt the flow of the photogenerated current in the p^+ diffusion region. Despite the interruption of the photogenerated current flow, the proposed photodetector has high responsivity due to its photogenerated current amplification mechanism, as mentioned in the previous section. As shown in this figure, a maximum responsivity of the proposed device of larger than 2.5×10^2 A/W is obtained. This value is considerably higher than that of a p-n junction photodiode, which is typically lower than 1 A/W.(10) When the bias at the built-in transfer gate is 0 V (Fig. 6 (a)), the photocurrent, as a function of the illumination intensity, is similar to the I_{DS}-V_{DS} characteristics as the gate bias varies in the MOSFET. This means that the incident light acts as a gate bias. When the bias at the built-in transfer gate is 3.3 V (Fig. 6(b)), the photocurrent, as a function of illumination intensity, can hardly be observed. This means that the built-in transfer gate is able to control the photocurrent flow.

Figure 7 shows the variation of the drain current (I_{DS}) with the light power as a function of the incident-light wavelength. The wavelengths used in this measurement are 633 nm (red), 533 nm (green) and 473 nm (blue). In this figure, we can confirm that the photocurrent is proportional to the light power for these three wavelengths.

Figure 8 shows the variation of the drain current (I_{DS}) with the drain voltage (V_{DS}) as a function of the channel length of the proposed photodetector when the channel width is 1.0 μm. Figure 9 shows the variation of the drain current (I_{DS}) with the drain voltage (V_{DS}) as a function of the channel width of the proposed photodetector when the channel length is 0.6 μm. The light source is the same as that in the previous experiment, and the

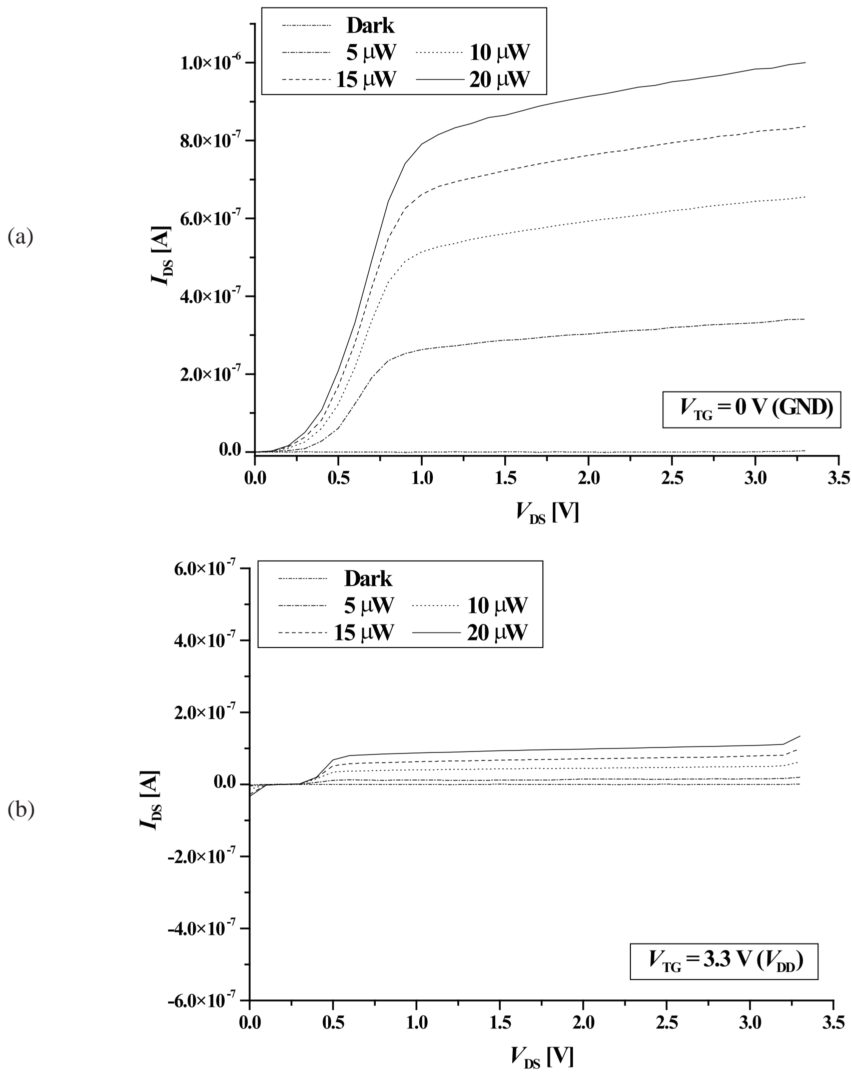

Fig. 6. Variation of the drain current (I_{DS}) with the drain voltage (V_{DS}) as a function of the incident-light power (wavelength = 633 nm): (a) bias of the transfer gate is 0 V and (b) bias of the transfer gate is 3.3 V.

light power is 20 μW. In these figures, we can confirm that the photocurrent increases with a decrease in the channel length and an increase in the channel width, since the photocurrent is proportional to the ratio of the channel width to the channel length of the MOSFET in this photodetector.

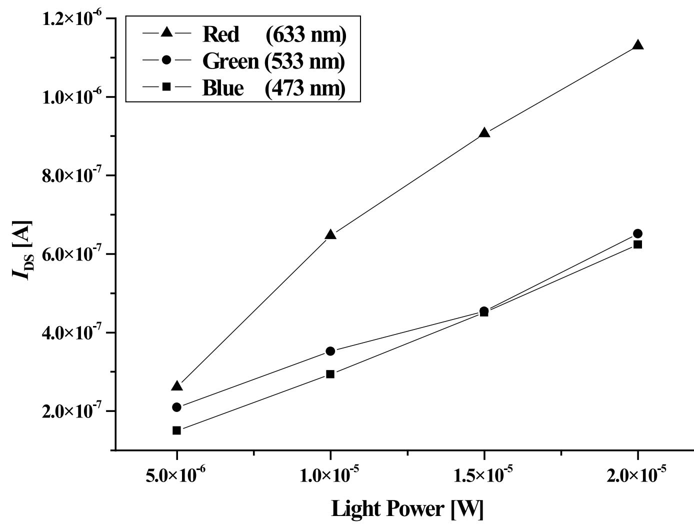

Fig. 7. Variation of the drain current (I_{DS}) with light power as a function of the incident-light wavelength.

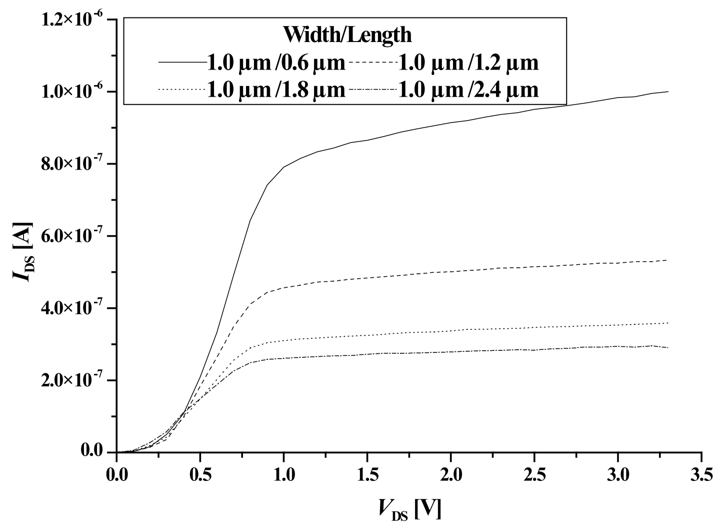

Fig. 8. Variation of the drain current (I_{DS}) with the drain voltage (V_{DS}) as a function of the channel length (channel width = 1.0 µm).

4. Conclusion

A novel n-well/gate-tied PMOSFET-type photodetector with a built-in transfer gate has been presented. The structure of the proposed photodetector is similar to that of the gate/body-tied PMOSFET photodetector. The proposed photodetector, however, has

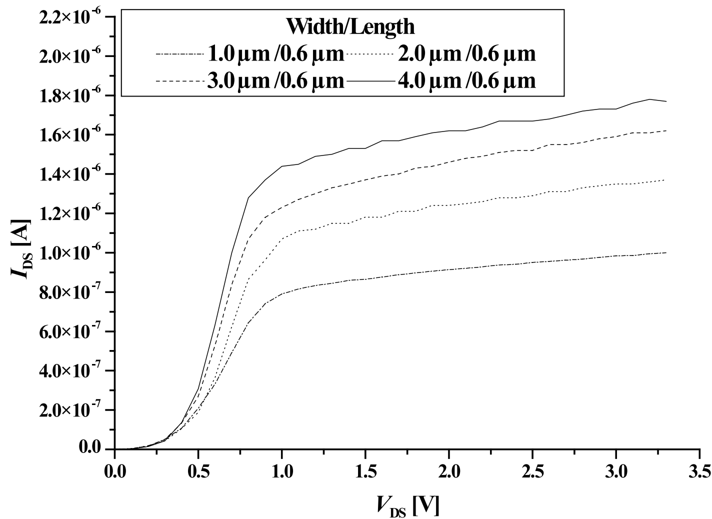

Fig. 9. Variation of the drain current (I_{DS}) with the drain voltage (V_{DS}) as a function of the channel width (channel length = 0.6 µm).

another gate that can control the generated photocurrent. The proposed photodetector has good optical characteristics with a photocurrent of about 1 µA. We could confirm the function of the built-in transfer gate from the measured results. This means that the proposed photodetector can control the photocurrent without using an additional MOSFET. Therefore, using the proposed photodetector, we can design a new pixel that occupies a smaller area than that of conventional CIS pixels.

Acknowledgements

This work was supported by Grant No. RT104-03-02 from the Regional Technology Innovation Program of the Ministry of Commerce, Industry and Energy (MOCIE) and the BK21 program in Korea.

References

1 M. Bigas, E. Cabruja, J. Forest and J. Salvi: Microelectron. J. **37** (2006) 433.
2 E. R. Fossum: IEEE Trans. Electron Devices **44** (1997) 1689.
3 M. Ogata, T. Nakamura, K. Matsumoto, R. Ohta and R. Hyuga: IEEE Trans. Electron Devices **38** (1991) 1005.
4 T. Lulée, S. Benthien, H. Keller, F. Mütze, P. Rieve, K. Seibel, M. Sommer and M. Böhm: IEEE Trans. Electron Devices **47** (2000) 2110.
5 K. Yonemoto and H. Sumi: IEEE J. Solid-State Circuits **35** (2000) 2038.
6 A. Rochas, A. R. Pauchard, P. A. Besse, D. Pantic, Z. Prijic and R. S. Popovic: IEEE Trans. Electron Devices **49** (2002) 387.

7 L. Laih, T. Chang, Y. Chen, W. Tsay and J. Hong: IEEE Trans. Electron Devices **45** (1998) 2018.
8 H. Zimmermann, B. Müller, A. Hammer, K. Herzog and P. Seegebrecht: IEEE Trans. Electron Devices **49** (2002) 334.
9 W. Zhang and M. Chan: IEEE Trans. Electron Devices **48** (2001) 1097.
10 H. Zimmermann: Sens. Mater. **13** (2001) 189.